PERGAMON

Deep-Sea Research I 49 (2002) 1485–1505

DEEP-SEA RESEARCH
PART I

www.elsevier.com/locate/dsr

# Intense mid-slope resuspension of particulate matter in the Faeroe–Shetland Channel: short-term deployment of near-bottom sediment traps

Jérôme Bonnin*, Wim van Raaphorst, Geert-Jan Brummer, Hans van Haren, Hans Malschaert

*Royal Netherlands Institute for Sea Research (NIOZ), P.O. Box 59, 1790 AB Den Burg, The Netherlands*

Received 16 July 2001; received in revised form 10 January 2002; accepted 9 April 2002

**Abstract**

An array of four moorings was deployed on a transect perpendicular to the south-eastern slope of the Faeroe–Shetland Channel to measure near-bottom fluxes during a 12-day period in spring 1999. Each mooring combined current meters and two sediment traps equipped with optical backscatter sensors (OBS) situated at 2 and 30 m above the bottom, at water depths of 470, 700, 800 and 1000 m. During the deployment, near-bottom current velocities at 470, 700 and 800 m water depth increased abruptly to values as high as 55 cm $s^{-1}$ (within a few hours). The sudden change in the cross-slope component of the current at 470 m was immediately followed by a severe drop in temperature at this depth, and large fluxes were intercepted in the mid-slope traps (700 and 800 m) on the same day, probably associated with the strengthening of the along-slope component. Organic carbon and nitrogen content of the trap samples were, except for the shallowest mooring, much lower than in particulate matter suspended in the water column. During the high flux event, particles possessed lower organic carbon and nitrogen values than during lower flux periods. This indicates that sedimentary material entered the traps. A simple multi-component mixing model was applied to the trap samples to estimate the relative contribution to our total mass fluxes of material from different sources: primary settling from the water surface, rebound material, and the relatively aged sediment. It showed that fluff was the main contributor to the resuspended flux but that sediment proper was resuspended at mid-slope during the strong increase in the current velocities and represented up to 70% of the total mass flux at that time. This study shows that near-bottom resuspension on the slope may be intense and, although the scale is here short-term the phenomena described might be larger in time and space. 

*Keywords:* Continental slope; Resuspension; Near-bottom sediment traps; Bottom Nepheloid layer; Faeroe–Shetland Channel; 60°30′N 2°W–61°30′N 5°W

## 1. Introduction

Although continental margins form only 11% of the world ocean surface area, more than 20% of the global primary production takes place there (Wollast, 1991) making them a key study area for organic carbon budget investigations. Large multi-disciplinary programmes conducted in the recent past have shown the importance of the continental slope, the boundary zone connecting the productive shelf to the deep ocean, to the global budget of

*Corresponding author. Fax: +31-222-319-674.
*E-mail address:* bonnin@nioz.nl (J. Bonnin).

0967-0637/02/$ - see front matter 
PII: S0967-0637(02)00030-4

particulate matter: SEEP I and II at the Middle-Atlantic Bight (Walsh et al., 1988; Biscaye et al., 1994; Biscaye and Anderson, 1994), OMEX I at Goban Spur (Van Weering et al., 1998), OMEX II at the western Iberian margin (Van Weering and de Stigter, 1999; Antia and Peinert, 1999; Epping et al., 2002) and ECOMARGE in the Gulf of Lions (Monaco et al., 1987, 1990a, b). These studies pointed out that particle flux to the slope sediment is mainly supplied by lateral transport from the shelf break rather than by pelagic settling. Nevertheless the final conclusion of the SEEP I and II programmes, i.e. the presence of a mid-slope organic carbon depocentre, was not validated by the observations during OMEX.

Erosion at the shelf edge and upper slope may be caused by strong boundary currents (Thomsen and Van Weering, 1998; Durrieu de Madron et al., 1999a) or be related to tidal motions (Vangriesheim and Khripounoff, 1990). It was also argued that short-term processes, like the breaking of internal waves on the slope, can cause substantial resuspension of sea floor material and generate detachment from the bottom of intermediate nepheloid layers (INL), which spread offslope along isopycnal surfaces (Dickson and McCave, 1986; McCave, 1986; Thorpe and White, 1988; Durrieu de Madron et al., 1999b; Van Raaphorst et al., 2001). These INLs are dynamic and intermittent features (Dickson and McCave, 1986; Van Raaphorst et al., 2001), whose occurrence and geographical extent may vary on short time-scales.

Here we present results from the PROcesses at the Continental Slope (PROCS) programme, carried out in the Faeroe–Shetland Channel (FSC), where we deployed four sets of moorings on a transect across the Shetland side of the channel (Fig. 1). On the mooring, sediment traps were deployed as close to the bottom as possible and equipped with optical backscatter sensors, current velocity meters and temperature sensors to determine hydrodynamical and sedimentological changes near the sea bed. Resuspension on slopes has been related to long-term fluctuations of along-slope currents (e.g. Thomsen and Van Weering, 1998) as well as to breaking of internal waves (Gardner, 1989a) and impingement of mesoscale features such as atmospheric perturbations and eddies (Gardner and Sullivan, 1981; McCave, 1986). Previous work in this area showed that the narrowness, the gentle facing slopes and the strongly stratified water column are favourable for the creation and reflection of internal waves (Sherwin, 1991). Van Raaphorst et al. (2001) showed that episodic nepheloid layers occur on the Shetlands slope at around 600 m depth. Therefore, we deployed our moorings close to one another on a transect across the slope with the sediment traps closely spaced above each other (28 m) to carefully look at the cross-slope zonation of resuspension/erosion. Although many authors have considered internal waves to be a possible mechanism for triggering sediment resuspension (Dickson and McCave, 1986; Thorpe and White, 1988; Gardner, 1989a, b), very few have quantified their impact in terms of particle resuspension and redistribution across the slope. Also, sediment traps have been intensively used during the last 2 decades to measure the vertical flux of sea surface derived particles to the bottom (Monaco et al., 1987; Biscaye et al., 1994; Biscaye and Anderson, 1994) and to measure resuspension and rebound fluxes in the deep oceanic environment (Gardner et al., 1983; Walsh et al., 1988). To our knowledge, nobody has used sediment traps to determine the resuspension of seabed material with a high time-resolution in an area influenced by internal waves and strong currents. This near-bottom sediment trap study across the continental slope is a first step towards such quantification. A simple end-member mixing model, based on particulate organic carbon and nitrogen contents, will be applied to determine the relative contribution of particles from different sources to our trap fluxes.

## 2. Characteristics of the study area

The FSC is located 60°N, 6°W to 63°N, 1°W and connects the Norwegian Sea with the North Atlantic and the Iceland Basin (Fig. 1). The shelf break is situated at about 200 m depth and in the axis the channel is about 1200 m deep. The Shetlands margin slope is gentle (<1%), about 50 km wide, and devoid of canyons. The sediment

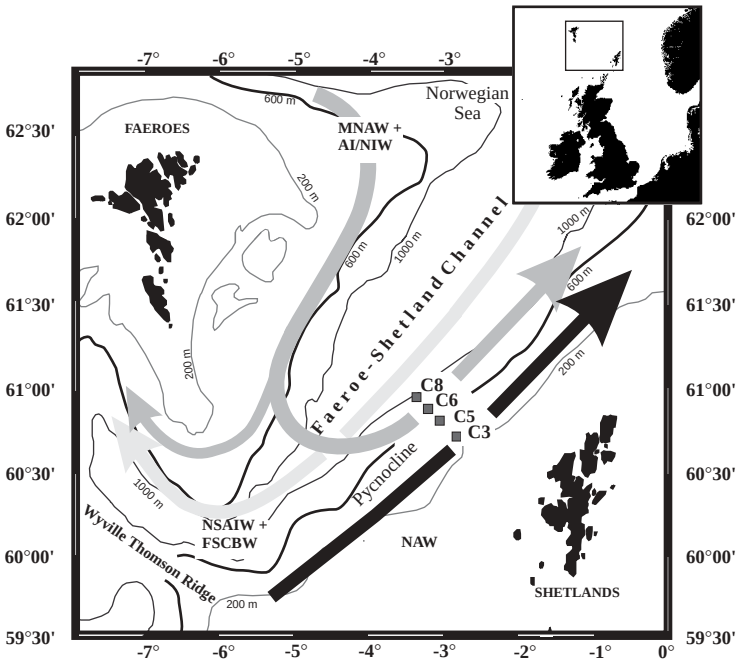


Fig. 1. Map of the study area with position of the moorings and trajectories of the main water masses in the Faeroe–Shetland Channel. The five water masses described by Turell et al. (1999) are grouped here into three according to direction of flow. Black arrow: North Atlantic Water (NAW), dark grey arrow: Modified North Atlantic Water (MNAW) and Arctic Intermediate/North Icelandic Water (AI/NIW), and light grey arrow: Norwegian Sea Arctic Intermediate Water (NSAIW) and Faeroe–Shetland Channel Bottom Water (FSCBW). The black line at 600 m represents the position of the major pycnocline where it intersects the bottom. For more details on the location of the moorings, see Table 1.

distribution follows the isobaths, with hard sands in a band between 300 and 450 m, glacial gravel and pebbles (median grain size $\sim$400 μm) in a band between 450 and 600 m, and finer muddy sands (median grain size $\sim$150 μm) covering the slope to the deepest part of the channel (Stoker et al., 1993). The average particulate organic carbon (POC) and particulate organic nitrogen (PON) content (% dw) for surface sediment are 0.28% and 0.04%, respectively (Table 1) with an average C/N ratio of 6.9. The POC and PON values for total particulate matter (TPM) are given in Table 2.

The FSC has a complex hydrography comprising five different water masses flowing in three layers on the eastern side of the channel (Turell et al., 1999). The surface waters, whose main component is the North Atlantic Water (NAW), flow from south-west to north-east. The intermediate waters are made of two components: one occupies a band across the channel at a depth between 300 and 700 m and flows from south-west to north-east (MNAW), and the other one (AI/NIW) flows from north-east to south-west at a depth between 600 and 800 m (Fig. 1 or see Turell et al., 1999 for more details). Finally, the bottom waters flow from north-east to south-west and comprise the Norwegian Sea Arctic Intermediate Water (NSAIW) and the Faeroe–Shetland Channel Bottom Water (FSCBW). The main thermocline is found between 400 and 600 m and shows its steepest gradient at $\sim$550 m (Fig. 2a and c). Vertical turbidity profiles (Fig. 2b and d) of the water column show rather low values in the upper photic zone, clear water below the thermocline and an increased turbidity in the vicinity of the sea bed (the bottom nepheloid layer: BNL). Clear water maximum is observed during days 117–118 on the

Table 1
Position and water depth of the moored sediment traps, median grain size with % of particles $<10\,\mu m$ (within brackets), POC and PON contents and POC/PON atomic ratio of surface sediments (0–2.5 mm depth interval)

| Trap number | Location of the moorings | Water depth (m) | Surface sediment median grain size (μm) | Surface sediment POC content (% dw) | Surface sediment PON content (% dw) | Surface sediment POC/PON |
|---|---|---|---|---|---|---|
| C3-30 | 60°48.48′N, −02°59.34′W | 470 | 400 (8) | 0.27 | 0.043 | 6.3 |
| C3-2 | — | | | | | |
| C5-30 | 60°55.36′N, −03°05.88′W | 700 | 144 (17) | 0.28 | 0.057 | 4.9 |
| C5-2 | — | | | | | |
| C6-30 | 60°56.91′N, −03°13.22′W | 800 | 185 (15) | 0.29 | 0.033 | 8.8 |
| C6-2 | — | | | | | |
| C8-30 | 61°00.09′N, −03°18.39′W | 1000 | 149 (13) | 0.27 | 0.036 | 7.5 |
| C8-2 | — | | | | | |

Table 2
POC and PON content of the total particulate matter (TPM) in the water column and close to the bottom (~5 mab) for different depths of the overlying water column

| Water depth (m) | POC content (% dw) of TPM | Standard deviation (number of samples) | PON content (% dw) of TPM | Standard deviation (number of samples) |
|---|---|---|---|---|
| 0–20 | 10.0 | 5.1 (27) | 0.67 | 0.23 (27) |
| 50–150 | 5.9 | 2.9 (28) | 0.13 | 0.09 (28) |
| 200–500 | 5.0 | 2.2 (54) | 0.09 | 0.07 (52) |
| 600–900 | 4.0 | 1.6 (15) | 0.06 | 0.05 (13) |
| Bottom <500 m | 3.9 | 2.2 (10) | 0.07 | 0.05 (7) |
| Bottom 500–700 m | 3.3 | 1.2 (6) | 0.07 | 0.06 (6) |
| Bottom 700–900 m | 4.7 | 2.2 (3) | 0.05 | 0.03 (3) |
| Bottom >900 m | 4.3 | 2.0 (10) | 0.06 | 0.02 (9) |

Shetland side (dark blue to purple on Fig. 2b) and maximum turbidity is observed on both sides during days 111–112. On the Shetland side, for the two sections, the near bottom turbidity is maximum at mid-slope and minimum on the upper slope. The Faeroe side is even more turbid than the Shetland one. Fig. 2 also gives us information on the dynamics of the BNL which was thicker and denser on days 111–112 than on days 117–118.

## 3. Material and methods

Four moorings, C3, C5, C6 and C8, including two sediment traps and four current meters each were deployed on a transect perpendicular to the Shetland margin at bottom depths of 470, 700, 800 and 1000 m, respectively (see Table 1 for coordinates). Sediment traps were positioned with their apertures at 2 and 30 m above the bottom (mab). They are hereafter identified by the number of the mooring followed by the height above the bottom at which they stand, for instance C5-2 and C5-30 for mooring C5 at 2 and 30 mab, respectively.

### 3.1. Sediment traps and trap samples treatment

Two types of sediment traps were used in this study: Technicap PPS 4/3 traps with 12 collecting cups (250 ml) were used for moorings C3, C5, C6 and trap C8-30, and a Kiel-type HDW trap with 20 collecting cups (250 ml) was used for trap C8-2. All PPS traps collected for 12 synchronised intervals of 24 h starting on April 19 0:00 h

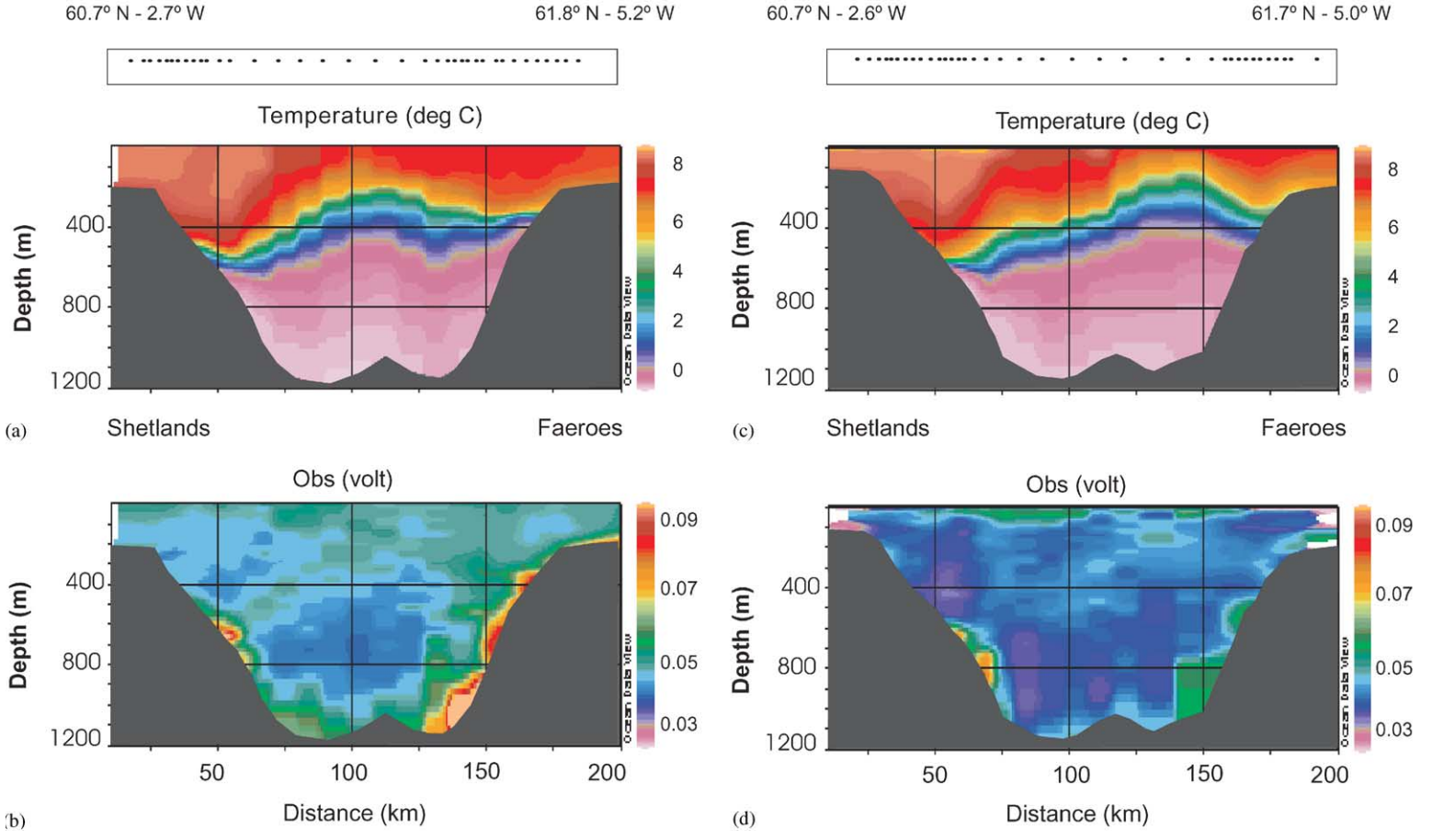


Fig. 2. Temperature (plots a and c) and turbidity (OBS) (plots b and d) section across the Faeroe–Shetland Channel on days 111–112 (plots a and b) and days 117–118 (plots c and d) obtained from CTD casts. The dots in the rectangles on top of the plots indicate the position of the measuring stations. This cross-section shows the strong temperature gradient in the channel and the enhanced turbidity at mid-slope on the Shetland side. Note also that, to some extent, the turbidity follows the position of the pycnocline.

(day108) and ending on April 30 24:00 h UTC (day 120). The HDW trap was programmed so that the initial eight collecting intervals could be covered by 16 intervals of 12 h, providing a more detailed record of the particle flux, followed by four intervals of 24 h. For each mooring the trap at 2 mab was mounted on a NIOZ-designed anchor frame, which allowed the sediment traps to be as close as possible to the sea bed. This frame, including weight and acoustic release system with a total weight under the water of 800 kg, effectively reduced the motion of the line. However considerable tilt was still observed in the bottom trap at 700 and 800 m (see Section 5.2) indicating movement of the anchor frame at very high current speed. To allow sampling in the high-energy regime of the FSC, all traps were modified from their conventional conical shape to cylindrical shape by adding a 1.5 m long PVC cylinder with baffled aperture (10 mm hexagons). The resulting total length of the effectively cylindrical traps is 2 m and the collecting area on the top of the trap is 0.042 $m^2$ (aspect ratio 8). Thus, all sediment traps have a similar collection area and a uniform shape. Cylindrical traps with high aspect ratio are appropriate to moderate energy conditions (Gardner, 1985) but still may give biased results in high-energy fields (Butman, 1986a, b; Gust et al., 1994), and we are aware of these problems.

The additional PVC cylinder mounted on trap C3-30 was lost at some unknown time during deployment, making it difficult to compare its fluxes with those of the other traps.

Prior to deployment, all collecting cups were filled with a mixture of seawater taken from the deployment site and depth, $HgCl_2$ (0.50 g $l^{-1}$) as biocide to prevent organic matter degradation and a pH-buffer ($Na_2B_4O_7 \cdot 10H_2O$; 2.00 g $l^{-1}$) to minimise carbonate dissolution. All programmed samples were recovered except cup number 5 of trap C3-2, which was filled but lost during recovery. After retrieval of the moorings, the trap samples were stored at 4°C until further processing at the NIOZ. The first sample of trap C8-2 was not processed as it was heavily contaminated with numerous badly preserved amphipod swimmers.

All samples were inspected with a binocular microscope, and swimmers, when present, were hand-picked. Total suspended matter was determined after filtration of the residue in the collecting cups through pre-weighted Poretics® polycarbonate filters (47 mm ∅, 0.4 μm pore size). When the amount of material was too large to be processed directly, the samples were split (up to 1/16th for the 5th sample of trap C6-2) before filtration with a manual roto splitter. The loaded filters were rinsed with 2 ml milli-Q water to remove the salts and frozen at −20°C, then freeze-dried and finally weighed after being exposed for at least 24 h in a humidity-controlled chamber of 30% relative humidity (Van Raaphorst et al., 2001).

### 3.2. Particulate organic carbon and nitrogen measurements

POC and PON content of the sediment trap samples was determined with a Carlo Erba NA 1500 Analyser according to the procedure described by Verardo et al. (1990) modified by Lohse et al. (2000). The samples were carefully scraped from the filters and crushed in an agate mortar. Inorganic carbon was removed from the samples by progressive and controlled acidification with sulphurous acid. The precision is ±0.3% for organic carbon and ±1.6% for nitrogen. Only the samples from moorings C5, C6 and C8 were fully analysed. The amounts of material collected in traps C3-30 and C3-2 were too small to allow C and N measurements for each sample. No samples were analysed for trap C3-30, and the 12 samples from trap C3-2 were pooled into five larger samples.

### 3.3. Current meters, tilt meters and optical backscatter sensors

Aanderaa RCM-8 current meters, including temperature sensors, were sampling once every 60 s and were moored at 8, 21, 34 and 47 mab on each mooring line, but here we will report only those closest to the sediment traps, at 8 mab. Accuracy of the current data based on 10-min ensembles is ±1 cm $s^{-1}$ and ±5° for speed and direction, respectively. Currents are positive to the north-east for the along slope component and

positive to the north-west (downslope) for the cross-slope component. To provide indication of the motion of the sediment traps, they were all equipped with NIOZ-designed tilt meters with an accuracy of 0.2° that sampled every 4 min.

Seapoint STM optical backscatter sensors (OBS) were mounted on the sediment traps to measure infrared light (wave length 880 nm) scattered by particles at angles between 15 and 150°. Calibration was performed by comparison with the total suspended matter concentration in the near-bottom water column sampled during CTD rosette (also equipped with OBS sensors) casts by filtration through Poretics® polycarbonate filters (47 mm ∅, 1.0 μm pore size). In addition we used sediment surface materials as well as sediment trap materials for calibration in the lab after the cruise. This showed that the OBS signal heavily depends on the particle size, in agreement with Bunt et al. (1999), who showed that optical devices are most sensitive to particles $<20\,\mu m$. Here, according to our estimates, it ranges from $1\,mg\,l^{-1}$ for 0.1 V measured by the OBS for fine material, to $3.4\,mg\,l^{-1}$ for 0.1 V for bulk surface sediment. On average, $1.8\,mg\,l^{-1}$ corresponds roughly to 0.1 V. Hatcher et al. (2001) argued that OBS sensors are not depending on particles size (dependent on mass) but on particle projected area concentration which, depending on fractal dimension, needs not to be proportional to mass. Nevertheless our calibration data are provided to give an estimation only, but to avoid any bias due to calibration, turbidity in this paper will be indicated in the original unit, i.e. Volt as measured by the OBS.

## 4. Results

### 4.1. Physical properties of the near-bottom water

The 2-week average near-bottom (8 mab) resultant current speed was 24.4, 20.5, 23.6 and $26.7\,cm\,s^{-1}$ at 470, 700, 800 and 1000 m, respectively (Fig. 3). The largest variability and highest maximum current speed occurred at 800 m water depth. The averaged along-slope velocity was directed north-east with values of 19, 9 and $8\,cm\,s^{-1}$ at 470, 700 and 800 m, respectively and southwest at 1000 m with a speed of $8\,cm\,s^{-1}$ (Fig. 4). Currents showed a high variability, with standard deviations ranging from 16 to $24\,cm\,s^{-1}$. Mean cross-slope currents were slightly directed upslope at mid-slope stations at velocities of $3\,cm\,s^{-1}$ at 700 and 800 m, and downslope at 470 and 1000 m with flow velocities of 2.8 and $0.2\,cm\,s^{-1}$, respectively. Standard deviations were 8–13 $cm\,s^{-1}$, less than for the along-slope direction. Current speed at stations C3, C5 and C6 (at 8 and 34 mab) decreased slightly from yearday 108 to 112, with a minimum on day 110, and then increased abruptly to reach a maximum value on day 112, showing high frequency current fluctuations close to the bottom. The velocity then diminished gradually to day 116 and strengthened again to the end of the record. At station C8, the velocity increased from day 108 to a maximum on day 109 then dropped gently to a minimum on day 117 and increased again with maxima on day 119. The oscillation signal was essentially semi-diurnal tidal (M2) for both the along-slope and cross-slope components at all the stations. Although our deployment time was too short to resolve the spring neap-tide cycle, we nevertheless observed variation with a period of 5–7 days during the deployment (Figs. 3 and 4). High frequency variations appeared immediately after the current reversal of the along-slope component at day 112, reflecting enhanced high frequency activity of the near-bottom water mass (see blow-up Fig. 4c). An abrupt temperature drop at 470 m water depth (Fig. 4b) is associated with this major current reversal. At station C5, the temperature variation in the first part of the record showed that the isotherms were moving up and down the slope. The peak on day 112 appeared to be related to the abrupt drop in temperature higher up the slope (station C3, 470 m). This peak was accompanied by an increase in the turbidity (Fig. 5f and g) as revealed by the optical backscatter sensors on the traps.

### 4.2. Total mass flux and turbidity

Microscopic observations revealed that the material found in all the traps during periods with

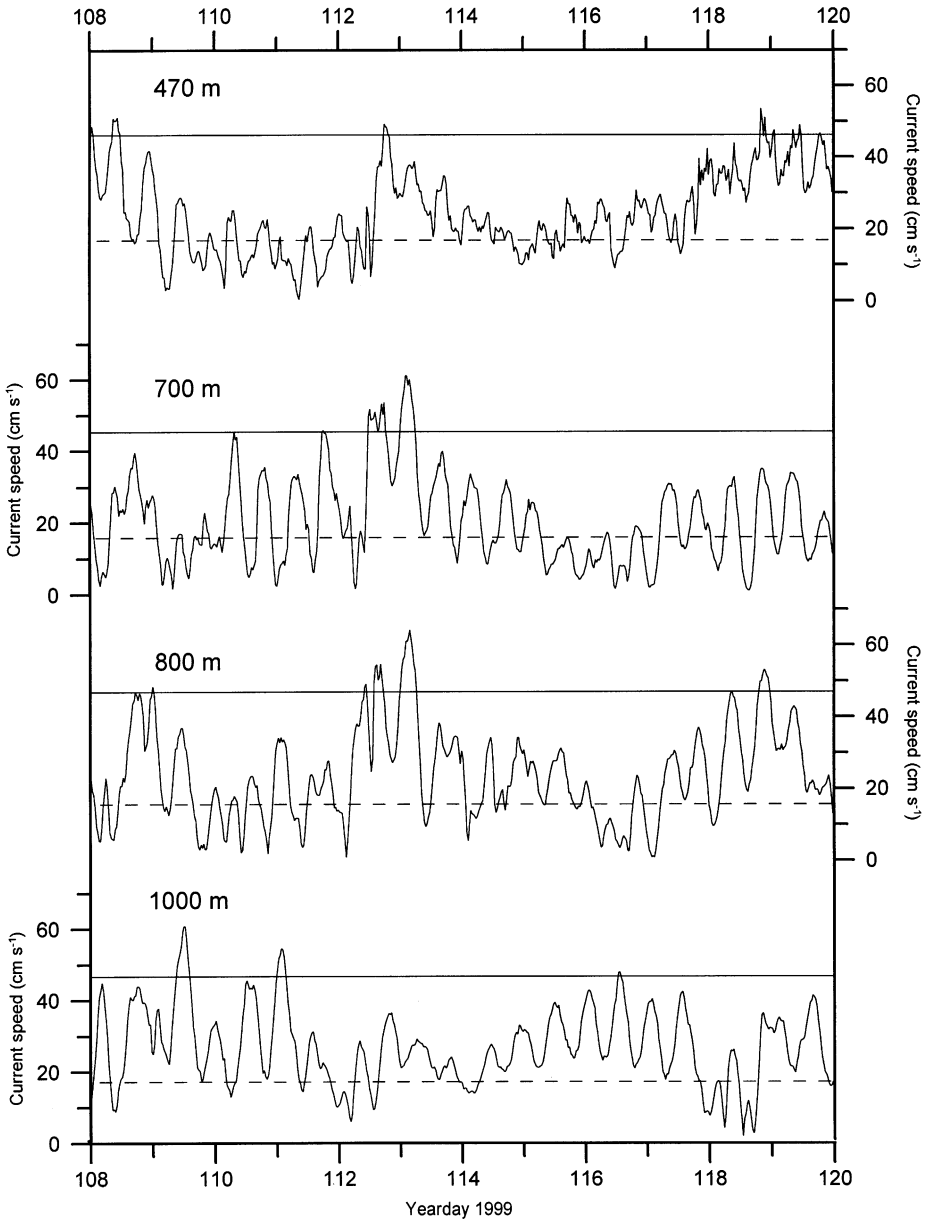


Fig. 3. Current speeds at 8 mab for the four moorings. The dashed line represents the threshold speed at which aggregates might be resuspended and the solid line the threshold erosion current speed for sediment proper.

relatively low mass fluxes consisted essentially of fluffy material composed of filaments, mucus and aggregates (reaching several mm in size), shells of planktonic forams (some still having their spines) and faecal pellets. However, during the high flux event (moorings C5 and C6) the material collected in the traps was composed mainly of lithogenic grains and planktonic and benthic forams embedded in a fluffy matrix suggesting a benthic origin of the particles.

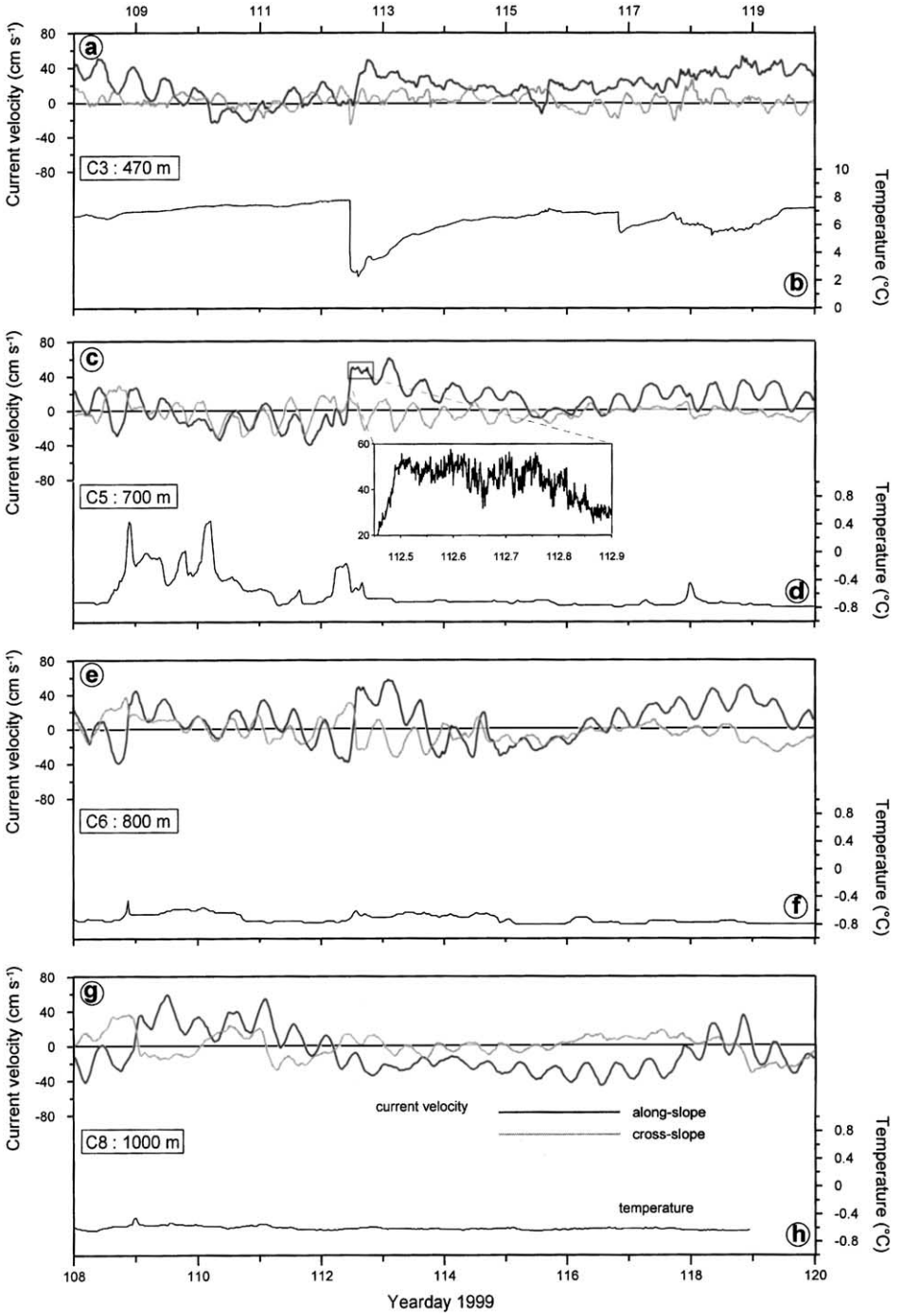


Fig. 4. Currents (a,c,e,g) and temperature (b,d,f,h) at 8 mab for the different stations. In plot a, c, e, g, the grey line represents the cross-slope component of the current (positive values orientated downslope) and the black line the along-slope component of the current (positive values to the north-east). The data shown here are 30-min averages. The blow up for station C5 shows the high frequency variations observed for the along-slope component (1-min averages) for 12 h during day 112.

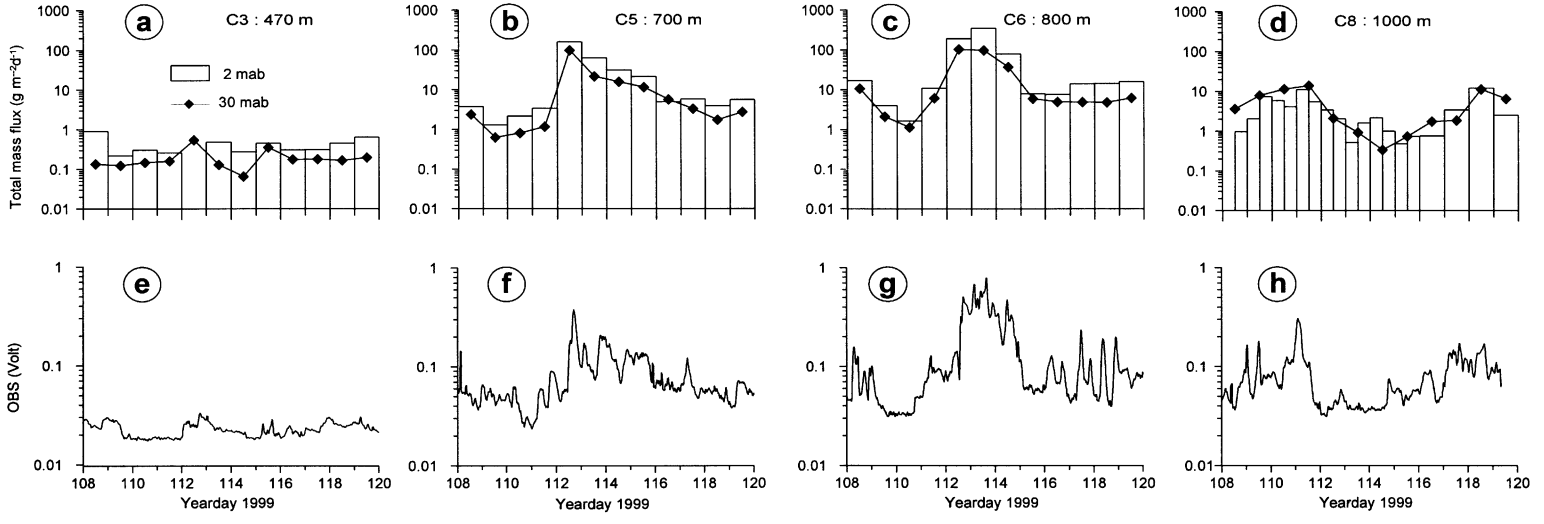


Fig. 5. Total mass fluxes in the sediment traps of the moorings C3, C5, C6 and C8 (plots a–d) for traps at 30 mab (line) and 2 mab (bars), and the turbidity (plots e–h) measured with the OBS sensors (2 mab) for each mooring.

The total mass flux (TMF) for every trap is given in Fig. 5(a–d). The intercepted fluxes closely follow the time series of the OBS (Fig. 5e–h). High TMF values correspond to high OBS values and vice versa, suggesting that the TMF recorded in the traps are directly related to the concentration of particles in the near-bottom water column. For moorings C3 (470 m), C5 (700 m) and C6 (800 m) TMF differed by a factor 2 between the upper trap (30 mab) and the lower trap (2 mab) suggesting input from resuspension of seafloor material at 2 mab. At the shallowest station, the TMF was very low both at 2 mab and at 30 mab (Fig. 5a). Even though the cylinder on top of trap C3-30 was lost during deployment thereby decreasing the aspect ratio from 8 to $<4$, its TMF matches well with those of trap C3-2. Traps of moorings C5 and C6 show comparable results with relatively low TMF during the first 4 days (days 108–111) followed by an abrupt increase at day 112 (Fig. 5b–c). Following this maximum on day 112, the TMF decreased gradually for mooring C5 (upper and lower traps) to reach background values again on day 116 (Fig. 5b). Farther downslope, trap C6-30 showed the same pattern as traps C5-2 and C5-30 while trap C6-2 showed a maximum on day 113 rather than on day 112 (Fig. 5c). At the deepest station (Fig. 5d), the TMF pattern was completely different as both upper and lower traps showed minimum fluxes during days 112 and 113 and maximum fluxes during days 111 and 118. Also in contrast to the other moorings higher on the slope, both traps of this mooring showed similar averaged TMF.

### 4.3. Organic carbon and nitrogen

High POC and PON content was observed when TMF in the traps was low and vice versa (Fig. 6a–f), suggesting that high TMF may be due to resuspension of organic-poor sediments (Table 1). For C5, C6 and C8, the POC content ranged from 0.36% to 3.89% and PON from 0.04% to 0.61%. For mooring C5 (700 m), maxima in POC and PON in bottom trap samples led those in the upper trap by one day. At mooring C6, the two traps displayed a synchronous signal of POC and PON. The POC and PON content are very similar to those in traps C5-2 and C5-30 situated 100 m higher on the slope. For mooring C8 we observed a lag of 2 days for the bottom trap for the maximum in both POC and PON (occurs on day 114 for trap C8-30 and on day 116 for trap C8-2).

## 5. Discussion

Given the distance of the sediment traps to the seabed and the energetic conditions in the near-bottom water column, we cannot assume that the trap fluxes indicate net vertical settling. Our main goal is to assess the relative intensity of resuspension of particulate matter across a high-energy continental slope and to investigate the quality of the intercepted material rather than to establish net sedimentation rates. During the last 2 decades, sediment traps have been used intensively to study long-term (seasonal) fluxes of particles onto the continental slope e.g. the Gulf of Lions in the Mediterranean (Monaco et al., 1990a, b), the Middle-Atlantic Bight (Biscaye et al., 1994), the Goban Spur at the mid-European continental margin (Antia et al., 1999). They have also been used to study near-bottom resuspension fluxes in various environments such as the north equatorial Pacific (Walsh et al., 1988), the western North Atlantic (Gardner et al., 1983; Gardner and Richardson, 1992), the northeast Atlantic (Lampitt et al., 2000) and the Oyster Grounds in the North Sea (Van Raaphorst et al., 1998). However sediment traps have not been used so far to study the short-term processes that determine the resuspension of bottom sediments and their redistribution across the continental slope.

### 5.1. Hydrodynamics and resuspension potential

Resuspension of bottom material is strongly linked with current velocity. Thomsen and Gust (2000) found that a flow speed of $45\,cm\,s^{-1}$ at 1 mab is necessary to initiate transport of sediment proper at the mid-slope continental margin of Goban Spur. Thomsen and Van Weering (1998) argued that currents about $20\,cm\,s^{-1}$ are sufficiently strong to resuspend periodically surface layer aggregates and Lampitt (1985) suggests that

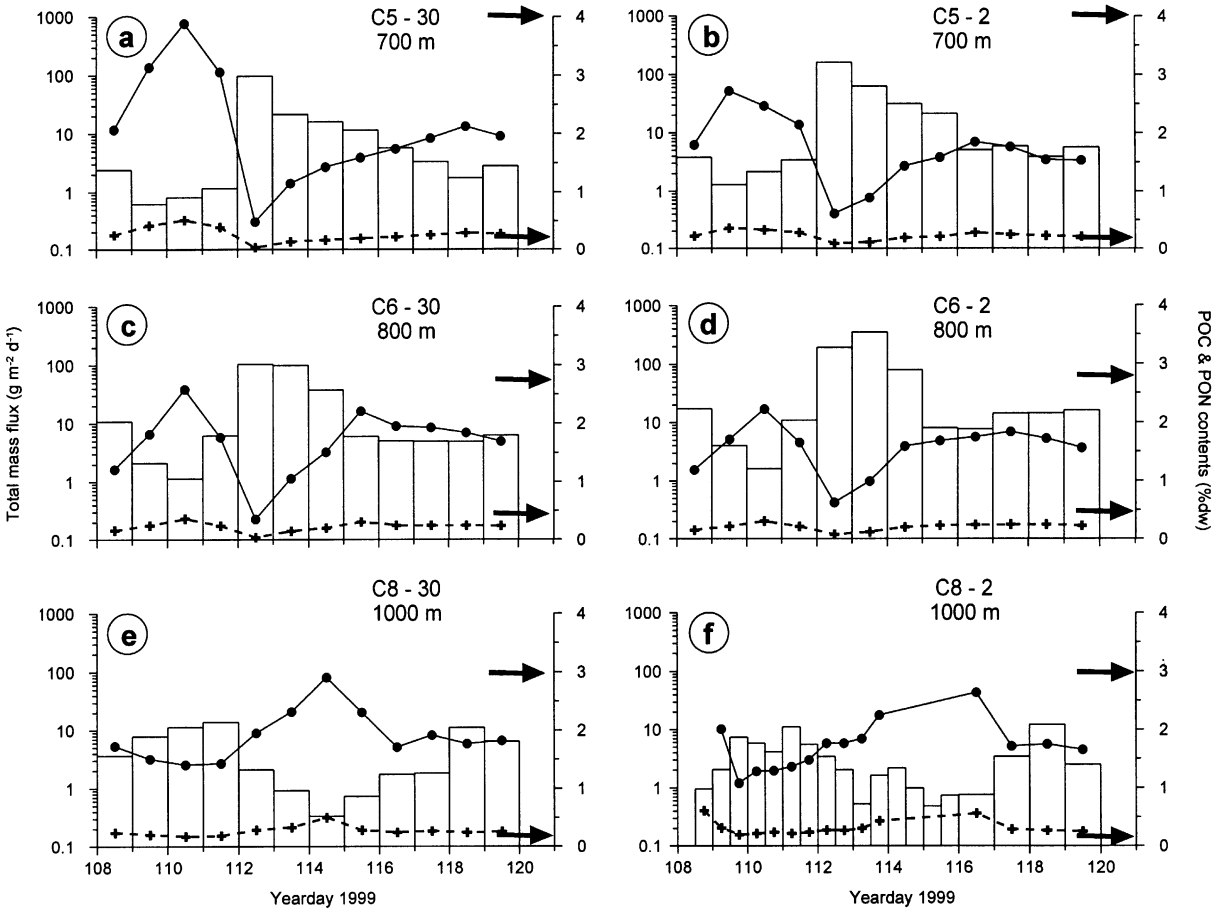


Fig. 6. POC (solid line) and PON (dashed line) content in % of dry weight of the total dry mass in the trap samples. The bars represent the TMF as shown in Fig. 5. For comparison, on each plot on the right side, the upper arrow represents the POC content of suspended particles in the near-bottom water (~5 mab) and the lower one the POC content of the surface sediment (0–2.5 mm depth interval).

currents $>7\,cm\,s^{-1}$ should resuspend a loose phytodetritus layer deposited on the deep-sea floor. For the North Sea, Van Raaphorst et al. (1998) determined that the threshold speed for resuspension of fluff is about $16\,cm\,s^{-1}$. In the Faeroe–Shetland Channel current speeds exceeded $7\,cm\,s^{-1}$ most of the time at all depths and currents $>45\,cm\,s^{-1}$ were also observed occasionally at all depths. Thus during most of the deployment time currents should be strong enough to erode a phytodetritus/aggregates layer when present and to keep it in suspension. Currents sufficiently high to erode the sediment proper ($>45\,cm\,s^{-1}$) also occurred at all depths but were restricted to a few days only.

Generally, higher turbidity was observed at higher current speeds and also the highest trap fluxes occurred on days with high current velocities. The deepest mooring, C8, which experienced, on average, slightly higher flow than on the upper slope, showed less turbidity and lower trap fluxes. The increase in turbidity and trap fluxes that took place on day 112 (moorings C5 and C6) appears to be due to resuspension generated by the strong reversal and intensification of the along-slope component. Van Raaphorst et al. (2001) observed a tidal shoaling of the major pycnocline in this area. The sequence on day 112 following the rapid upward motion of the pycnocline (observed down to 700 m) may be due to the passage of a

tidal bore, or any other high-energy event. We conclude that resuspension of fine particles can occur at all depths across the slope during the entire study period.

### 5.2. High trap fluxes and tilt effects

Tilt of sediment traps can result in either under or overestimation of the settling flux (Gardner, 1985; Gust et al., 1994). Tilt meters mounted on the traps revealed that the mid-slope traps had been tilted up to 36° (for trap C6-2) during the abrupt reversal in the current velocity on day 112 (Fig. 7), but that the average tilt was only 3.7°. Enhanced tilt was observed at current speeds over $30\,\mathrm{cm\,s^{-1}}$ whereas angles of more than 5° occurred at speeds above $50\,\mathrm{cm\,s^{-1}}$. Strong flow may cause enhanced exchange between the interior of the trap and the ambient water column but precautions to minimise this effect were taken by extending the aspect ratio of the sediment traps prior to deployment. It can nevertheless be questioned whether the trap data indicate genuine resuspension fluxes or mainly reflect tilt effects.

Following Gardner (1985), a first order correction for the effect of tilt on collection efficiency was made on our trap fluxes with the sine function:

$$F = F_T \int_0^{\Delta T} \frac{1}{1 + 1.4 \sin 2\theta}\,\mathrm{d}t \quad \text{with}$$
$$\Delta T = 1\ \text{day (trap interval)}, \tag{1}$$

where $F$ is the corrected flux expected in a vertical cylinder, $F_T$ is the observed flux in a tilted cylinder and $\theta$ is the degree of tilt from the vertical. Strong flow may also generate shear at the mouth of the trap that leads to break-up of aggregates and

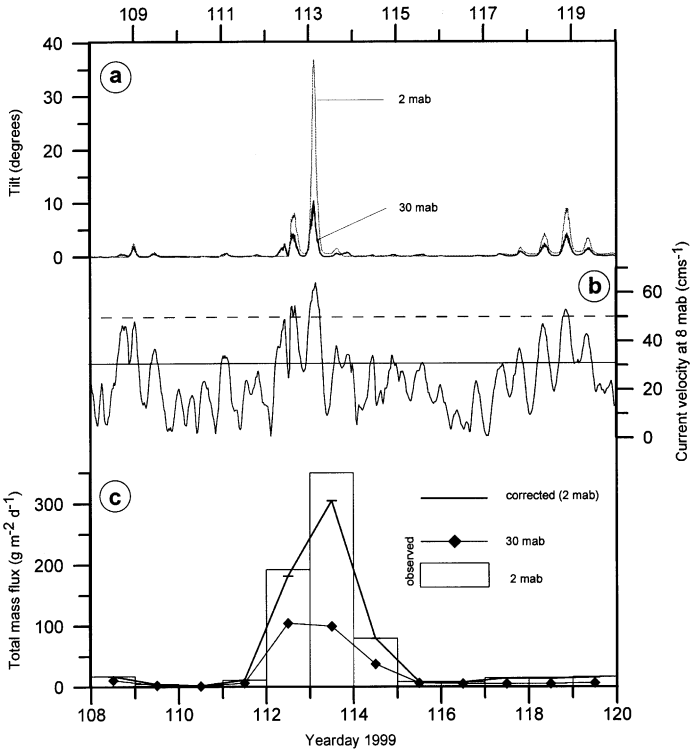


Fig. 7. Tilt of the traps from the vertical (a), current speed (b) and total mass flux (c) for trap C6-2. For total mass flux, the bar chart represents the intercepted flux by the trap at 2 mab, the line and diamonds the intercepted flux at 30 mab, and the solid line the corrected flux for trap C6-2 according to Eq. (1) from Gardner (1985).

undersampling of fine material. Although this phenomena is difficult to quantify, Eq. (1), based on empirical observations, partially correct this effect. Correction for the tilt effect for trap C6-2 gives slightly lower flux values than those measured (by 0.2–12.8% for the minimum and maximum tilt angle, respectively, Fig. 7c). Despite the relatively large tilt angles at some moments, the corrected fluxes show the same pattern as the uncorrected ones, and on day 113 the corrected flux of trap C6-2 remains very large ($305\,g\,m^{-2}\,d^{-1}$). High angles of tilt occurred during short periods only and their contribution to the integrated fluxes was therefore probably minor. Moreover, the correction is meant for sediment traps with an aspect ratio of $\sim 5$, and cylindrical traps with higher aspect ratio (8 in our case) are presumably less sensitive to tilt effects. This is also supported by the observation that during the times of strongest tilt, our sediment traps collected large amount of coarse and fast sinking particles (sand, foraminifera), which are much less affected by fluid motion in the traps (Gardner, 1985). Another argument in favour of a minor tilt effect on our flux estimates is the low TMF ($\sim 5\,g\,m^{-2}\,d^{-1}$) observed for example in trap C6-2 on days 118 and 119 for a tilt angle up to 10°, whereas with a similar tilt on day 112, a flux as high as $180\,g\,m^{-2}\,d^{-1}$ was intercepted. We conclude that the high fluxes in our traps are not due to tilt effects.

### 5.3. Temporal and spatial variability in the trap fluxes

High temporal variability of TMF was observed in almost all the traps. Small fluxes correspond to relatively low current velocities ($\sim 20\,cm\,s^{-1}$ in average) and high fluxes to stronger currents (up to $61\,cm\,s^{-1}$ 8 mab at 700 m water depth). At moorings C3, C5 and C6, the 2-fold higher TMF in the lower traps, relative to the upper ones, correspond to higher turbidity at 2 mab than at 30 mab, thereby confirming resuspen sion as a major source (Biscaye and Eittreim, 1977).

The average TMF of the mid-slope traps (C5 and C6) of $30.7\,g\,m^{-2}\,d^{-1}$ during the 12-day deployment is higher than what has been observed elsewhere in open continental slopes at similar depth. On the Eel continental slope, Walsh and Nittrouer (1999) found values of $11.8\,g\,m^{-2}\,d^{-1}$ at 15 mab (but with an important river discharge nearby), whereas Biscaye and Anderson (1994) found fluxes not higher than $10\,g\,m^{-2}\,d^{-1}$ at 10 mab during the SEEP I and II experiments in the Middle-Atlantic Bight. Our values are close to those observed in submarine canyons where Baker and Hickey (1986) found fluxes up to $200\,g\,m^{-2}\,d^{-1}$ a few meters above the bottom with an average of $60\,g\,m^{-2}\,d^{-1}$ at 450 m water depth. However, our deployment time is shorter than that of the studies cited above, which, considering that we caught an extremely high flux event, makes direct comparison difficult.

The cross-slope differences in TMF are considerable, as on average only $0.3\,g\,m^{-2}\,d^{-1}$ was captured at the shallowest station (C3), $5\,g\,m^{-2}\,d^{-1}$ at the deepest station (C8), and up to $160\,g\,m^{-2}\,d^{-1}$ (C5-2) and $350\,g\,m^{-2}\,d^{-1}$ (C6-2) at the mid-slope stations. This suggests that the mid-slope is far more active in terms of resuspension/deposition than the rest of the slope. Amin and Huthnance (1999) showed that a mid-slope source of resuspendable sediments is necessary to explain maximum concentration of particles in the BNL generally observed at this depth. The increase of the flux in the 700 and 800 m traps is intense and abrupt, with according to the OBS sensors mounted on the traps only a few hours between the minimum and maximum turbidity, suggesting a relatively nearby source for this short-term resuspension event. Also, coarse particles point at local source of resuspension.

### 5.4. Origin of the resuspended material

The sediments on the slope of the FSC are of glacial origin and composed mainly of coarse sands and gravel (Stoker et al., 1993), likely because the high bottom current speed in this region does not allow for a large sedimentary reservoir of fine and easily resuspendable particles. Moreover, The FSC is a mesotrophic area with a primary production ranging from 1.2 to $3.8\,g\,C\,m^{-2}\,d^{-1}$, with the lowest values in the

northern channel and the highest in the southern and middle channel (Riegman and Kraay, 2001). Although these primary production values are relatively high, primary settling associated with export fluxes from the euphotic zone cannot explain the largest fluxes of particles in our traps, although it may explain part of our background fluxes. According to Suess (1980) the above primary production may, on average, give deposition fluxes between 0.06 and 0.2 $g\,C\,m^{-2}\,d^{-1}$ at the sea bed at 700 m. This estimate is in good agreement with our background fluxes ($0.07\,g\,C\,m^{-2}\,d^{-1}$ at 700 m water depth) but certainly cannot explain fluxes orders of magnitude higher.

On the long term, local source for the fluxes intercepted in our near-bottom traps seems unlikely. A more likely explanation is that it is fuelled by lateral advection from further up-stream, possibly from the Wyville–Thomson Ridge, being transported by the strong contour currents. The particle-loaded water may migrate vertically on the slope from below the pycnocline to the bottom of the channel depending on the cross-slope velocity (Oey, 1998). The processes are thus not limited to a 2D cross section view but 3D interactions between along-slope and cross-slope mechanisms must be considered (Dickson and McCave, 1986; Biscaye and Anderson, 1994). Nevertheless, during periods of lower current speeds particles may preferentially accumulate temporarily on the mid-slope as indicated by increased $^{210}Pb$ (Van Raaphorst et al, 2001) and $^{234}Th$ inventories (Grutters et al., submitted) at 700–800 m depth until an event of higher flow velocity occurs as observed on day 112. We saw earlier that flow conditions at any depth on the slope should be capable of bottom material erosion. The absence of resuspension at mooring C3 (470 m) could be due to lack of material available for resuspension. Indeed, sediments at 470 m consist of coarse, hard sands with very little fine grains (less than 7% $<63\,\mu m$ in the upper 2.5 mm, Grutters et al., submitted). The coarser fraction of the resuspended particles probably settles out close to the point of erosion while the finer particles may settle further along-slope and down-slope. OBS transects across the FSC (Fig 2b) show distinct turbidity maximum on the Shetland slope between 550 and 900 m (just below the major pycnocline), suggesting that resuspension occurred within this depth interval on the slope. The reason why no resuspension of sediment proper was found at the deepest station may be that the major source of material is situated at shallower depth (above 850 m) and that the upslope flow does not allow particles to reach the deepest part of the channel.

### 5.5. Composition of resuspended flux

As suggested by Thomsen and Van Weering (1998), BNLs are partially sustained by refractory resuspended particles and partially by fresh labile aggregates, the so-called "rebound" flux (Walsh et al., 1988). Elemental analysis performed on our trap material yielded a negative correlation between TMF and their POC and PON contents. If we assume that the small amount of material collected in traps C3 reflects the primary flux reaching the seabed (which is probably already an overestimation, as a small amount of resuspension may take place here as well), the traps deeper down the slope, which intercepted much higher TMF, would mainly reflect resuspension. The time lag in the POC and PON signature between the upper and bottom trap of mooring C5 (700 m) also indicates that the material caught by the traps originated mainly from the seabed. At mooring C6, the two traps display a synchronous signal of POC and PON although a lag of one day with respect to the bottom trap is observed for the TMF. This suggests that the two traps of this mooring received material with a similar geochemical signature and may originate from the same place. Moreover, the POC and PON contents are very similar to those obtained in traps C5-2 and C5-30 situated 100 m higher up on the slope, indicating that material in the traps of these two moorings also has a similar source. For mooring C8 we observed a lag of 2 days for the bottom trap for both POC and PON maxima (occurring on day 114 for trap C8-30 and on day 116 for trap C8-2), which suggests, on the contrary, settling from an INL entrained higher up-slope.

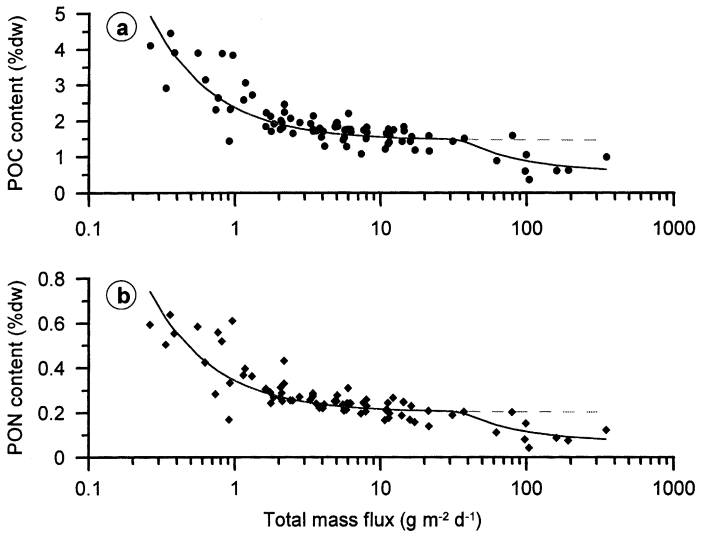


Fig. 8. POC (a) and PON (b) content versus total mass flux for the entire sediment trap data set. The dashed regression line represents Eq. (3) with values of $(C_0–C_r)S_0 = 0.90\,g\,m^{-2}\,d^{-1}$ and $C_r = 1.52\%$ for (a) and $(C_0–C_r)S_0 = 0.14\,g\,m^{-2}\,d^{-1}$ and $C_r = 0.20\%$ for (b). The solid line represents Eq. (6) with additional parameters $\alpha = 0.21$ for (a) and 0.04 for (b) and $C_b = 0.31\%$ for (a) and 0.06% for (b).

To determine whether the resuspended particles collected in our traps have similar properties as the top layer of the surface sediments or the suspended particles in the water column we follow the approach of Jago et al. (1993) and apply the two-component mixing model of Morris et al. (1987). In this model it is assumed that the TMF consists of a constant background (primary flux) $S_0$ with carbon content $C_0$, and a variable rebound flux $S_r$ having a carbon content $C_r$:

$$\mathrm{TMF} \times \mathrm{POC} = S_0 C_0 + S_r C_r. \quad (2)$$

Taking into account that the total mass flux $\mathrm{TMF} = S_0 + S_r$, we can substitute for $S_r$ in (2) and the POC content of the flux is then given by

$$\mathrm{POC} = (C_0 - C_r)\frac{S_0}{\mathrm{TMF}} + C_r. \quad (3)$$

From the regression of POC against TMF using the entire sediment trap data set, $C_r$ is calculated at 1.52% (Fig. 7). This is approximately 2.5 times lower than the average value of POC in particles in the near-bottom water column ($\sim$4%, see Table 2) and $\sim$5 times higher than the average content in the upper 2.5 mm of the sediments ($\sim$0.28%), and is in good agreement with Van Raaphorst et al. (1998) for the North Sea and with Lampitt et al. (2000) for abyssal conditions. They both found that particles that are resuspended during normal flow conditions are carbon-enriched compared to the bulk sediment suggesting that they are made up of aggregates that had recently arrived at the seafloor or were retained in the benthic boundary layer (BBL). However, the model cannot explain the low POC content at high TMF ($> \sim 35\,g\,m^{-2}\,d^{-1}$), indicating that two end members are not sufficient to explain the variability of our trap contents.

We incorporated a third component in the model to check whether the material present in our traps during high TMF events ($> 35\,g\,m^{-2}\,d^{-1}$) corresponds to bed material. We assume that trap samples for TMF $> 35\,g\,m^{-2}\,d^{-1}$ consist of the same rebound material found at fluxes up to $35\,g\,m^{-2}\,d^{-1}$, to which the material of the extra flux (assumed to be from sediment) is added. This is expressed by

$$\mathrm{TMF} \times \mathrm{POC} = 35\,\mathrm{POC}_{35} + S_b C_b' \ \text{for TMF} > 35 \quad (4)$$

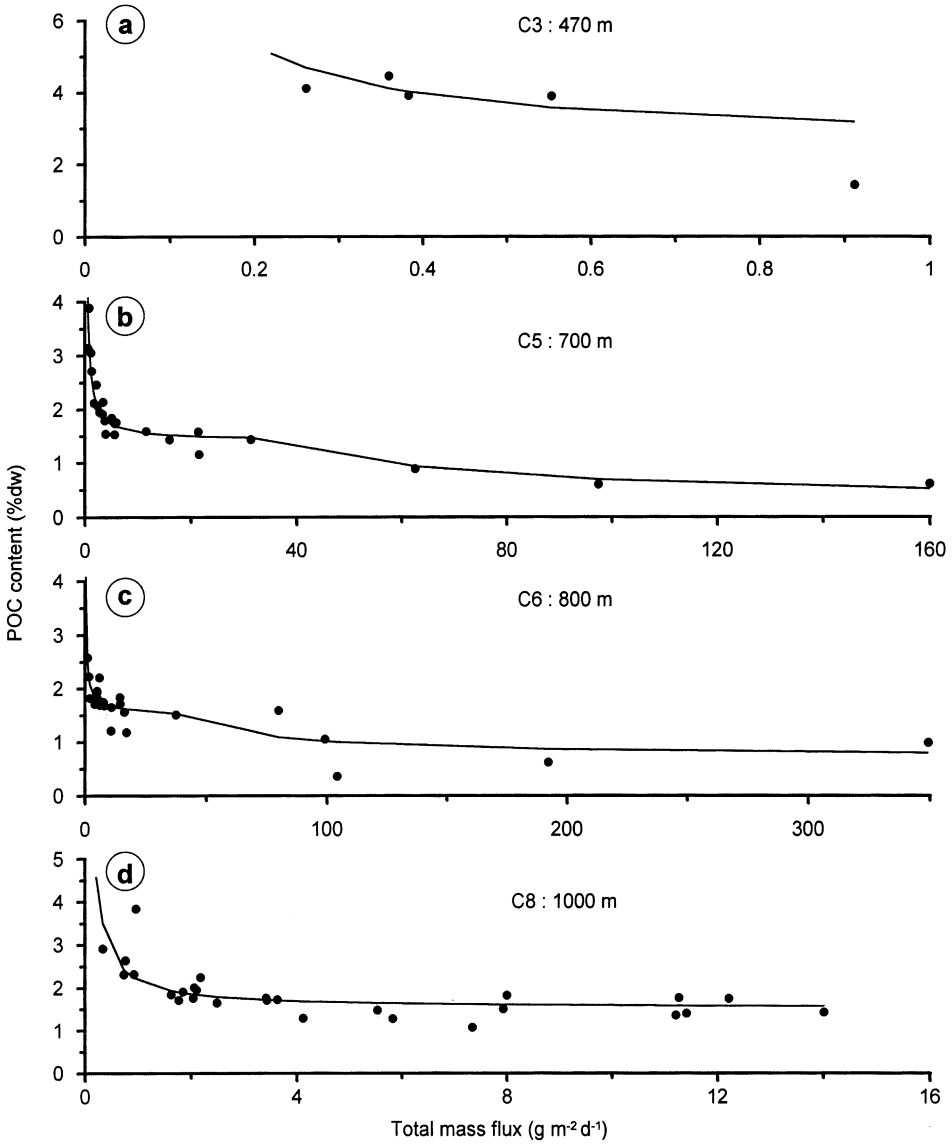


Fig. 9. POC content versus total mass flux for separate stations. For stations C3 and C8 the solid line represents regression line obtained from Eq. (3) with $(C_0–C_r)$ $S_0 = 0.5\,g\,m^{-2}\,d^{-1}$ and $C_r = 2.5\%$ for C3 and $(C_0–C_r)$ $S_0 = 0.66\,g\,m^{-2}\,d^{-1}$ and $C_r = 1.52\%$ for C8. For stations C5 and C6, the regression line represents the results of Eq. (6) with $(C_0–C_r)$ $S_0 = 1.53\,g\,m^{-2}\,d^{-1}$, $C_r = 1.42\%$, $\alpha = 0.07$, $C_b = 0.17\%$ for C5 and $(C_0–C_r)$ $S_0 = 1.10\,g\,m^{-2}\,d^{-1}$, $C_r = 1.55\%$, $\alpha = 0.25$, $C_b = 0.42\%$ for C6.

and

$$C'_b = \alpha C_r + (1-\alpha)C_b, \tag{5}$$

where $POC_{35}$ corresponds to the modelled POC content, from (3), at $TMF = 35\,g\,m^{-2}\,d^{-1}$, $S_b$ is the additional flux of resuspended sediments, $C'_b$ the POC content of the total resuspended particles at $TMF > 35\,g\,m^{-2}\,d^{-1}$, $C_b$ the POC content of surface sediments, $\alpha$ the percentage of rebound material of the resuspension pool in the trap

samples at TMF > 35 and $C_r$ the POC content of this rebound fraction (as in (2) and (3)). Knowing that TMF = 35 + $S_b$, we arrive at the equation for the POC content at TMF > 35:

$$\mathrm{POC} = \left[(C_0 - C_r)\frac{S_0}{35} + C_r\right] \times \left(\frac{35}{\mathrm{TMF}}\right) + \left(1 - \frac{35}{\mathrm{TMF}}\right) \times [\alpha C_r + (1-\alpha)C_b] \quad (6)$$

in which $\alpha$ and $C_b$ are the only additional unknown parameters. We obtained a POC content $C_b$ for the sediment end member of ~0.31%, which is very close to the surface sediment carbon content value (0.28% on average) and a mean value for $\alpha = 0.21$.

Although the model is more robust when applied to the entire data set (Fig. 8), we applied it to the individual stations as well. Fig. 9 shows that for the shallowest station (C3, 470 m) and the deepest station (C8, 1000 m) the 2-end-member model (Eq. (3)) fits well with the POC data. It reflects mainly the small primary flux for C3 and shows that rebound material is the main component of the flux at station C8. The two mid-slope stations show that the three component mixing model fits the POC data best (especially at 700 m). Fig. 10 shows the relative distribution of sediment proper relative to the TMF in the mid-slope traps as given by $\alpha$ obtained from Eq. (6). It shows that rebound material is the major component of the flux during the normal flow conditions but that sediment proper can enter the traps and constitute the major constituent during the periods of high current speed, representing up to 70% of the TMF at that time.

## 6. Conclusions

The fluxes intercepted in our traps were much higher than fluxes observed in other open slopes and mainly reflect resuspension of recently settled aggregates. During the 12-day deployment TMF was highest at mid-slope due to an admixture of

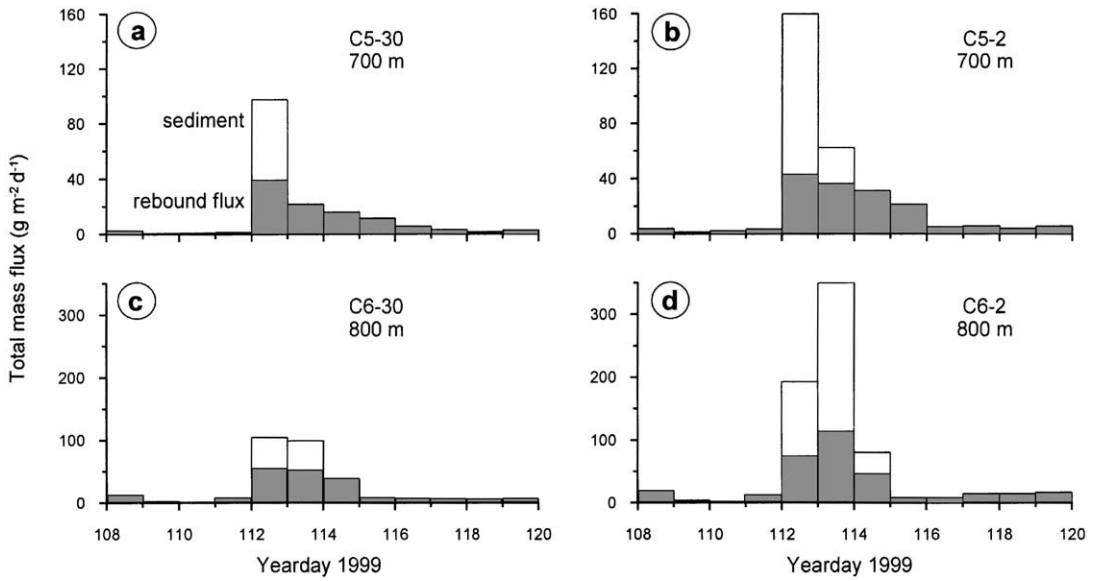


Fig. 10. Relative contribution of rebound particles (black) and sediment proper (white) to the total resuspension flux for the two mid-slope moorings. When TMF exceeded 35 g m$^{-2}$ d$^{-1}$, the relative contribution of rebound to the total mass flux is given by $\alpha$($\alpha = 0.07$ for C5 and 0.25 for C6). The primary flux remains within the thickness of the line of the $x$-axis.

material of sedimentary origin. The material in our traps constitutes then a mixture between: (1) the primary settling particles that represents the majority of the flux on the upper slope down to at least 470 m water depth and which we assumed to be constant ($\sim 0.3\,g\,m^{-2}\,d^{-1}$); (2) the rebound particles that have been already in contact with the surficial layer of the sediment or the BBL, less rich in Corg than the primary settling particles with which they constitute the background flux on the slope deeper than 470 m during normal current speed; and (3) sediments that are resuspended under the high current velocities (above $\sim 50\,cm\,s^{-1}$) at 700 and 800 m on days 112–114 and which represents up to 70% of the TMF during day of major resuspension event.

## Acknowledgements

We wish to thank the technicians and the crew of the R.V *Pelagia* for field assistance during the PROCS cruises and P. Hosegood for providing the current meter data. The helpful comments of three anonymous reviewers greatly improved the manuscript. The investigations were supported by the Research Council for Earth and Life Sciences (ALW) with financial aid from the Netherlands Organization for Scientific Research (NWO). This is NIOZ contribution No. 3652.

## References

Amin, M., Huthnance, J.M., 1999. The pattern of cross-slope depositional fluxes. Deep-Sea Research I 46 (9), 1565–1591.

Antia, A.N., Peinert, R., 1999. Particle flux at the Iberian Margin, Ocean Margin Exchange II Report, pp. 249–254.

Antia, A.N., von Bodungen, B., Peinert, R., 1999. Particle flux across the mid-European continental margin. Deep-Sea Research I 46, 1999–2024.

Baker, E.T., Hickey, B.M., 1986. Contemporary sedimentation processes in and around an active west coast submarine canyon. Marine Geology 71, 15–34.

Biscaye, P.E., Anderson, R.F., 1994. Fluxes of particulate matter on the slope of the southern Middle Atlantic Bight: Seep-II. Deep-Sea Research II 41, 459–509.

Biscaye, P.E., Eittreim, S.L., 1977. Suspended particulate loads and transport in the nepheloid layer of the abyssal Atlantic Ocean. Marine Geology 23, 155–172.

Biscaye, P.E., Flagg, C.N., Falkowski, P.G., 1994. The Shelf Edge Exchange Processes experiment, SEEP-II an introduction to hypotheses, results and conclusions. Deep-Sea Research II 41, 231–252.

Bunt, J.A.C., Larcombe, P., Jago, C.F., 1999. Quantifying the response of optical backscatter devices and transmissometers to variations in suspended particulate matter. Continental Shelf Research 19, 1199–1220.

Butman, C.A., 1986a. Sediment trap biases in turbulent flows: results from a laboratory flume study. Journal of Marine Research 44 (3), 645–693.

Butman, C.A., Grant, W.D., Stolzenbach, K.D., 1986b. Predictions of sediment trap biases in turbulent flows: a theoretical analysis based on observation from the literature. Journal of Marine Research 44 (3), 601–644.

Dickson, R.R., McCave, I.N., 1986. Nepheloid layers on the continental slope west of Porcupine Bank. Deep-Sea Research 33, 791–818.

Durrieu de Madron, X., Radakovitch, O., Heussner, S., Loye-Pilot, M.D., Monaco, A., 1999a. Role of the climatological and current variability on shelf-slope exchanges of particulate matter: evidence from the Rhone continental margin (NW Mediterranean). Deep-Sea Research I 46 (9), 1513–1538.

Durrieu de Madron, X., Castaing, P., Nyffeler, F., Courp, T., 1999b. Slope transport of suspended matter on the Aquitanian margin of the Bay of Biscay. Deep-Sea Research II 46, 2003–2027.

Epping, E., Van der Zee, C., Soetaert, K., Helder, W., 2002. On the oxidation and burial of organic carbon in sediments of the Iberian Margin and Nazaré canyon (NE Atlantic). Progress in Oceanography 52, 399–431.

Gardner, W.D., 1985. The effect of tilt on sediment trap efficiency. Deep-Sea Research 32 (3), 349–361.

Gardner, W.D., 1989a. Periodic resuspension in Baltimore Canyon by focusing of internal waves. Journal of Geophysical Research 94, 18185–18194.

Gardner, W.D., 1989b. Baltimore Canyon as a modern conduit of sediment to the deep sea. Deep-Sea Research 36, 323–358.

Gardner, W.D., Richardson, M.J., 1992. Particle export and resuspension fluxes in the Western North Atlantic. In: Rowe, G.T., Pariente, V. (Eds.), Deep-Sea Food Chains and the Global Carbon Cycle. Kluwer Academic Publishers, Dordrecht, pp. 339–364.

Gardner, W., Sullivan, L.G., 1981. Benthic storms: temporal variability in a deep-ocean Nepheloid layer. Science 213, 329–331.

Gardner, W.D., Richardson, M.J., Hinga, K.R., Biscaye, P.E., 1983. Resuspension measured with sediment traps in a high-energy environment. Earth and Planetary Science Letters 66, 262–278.

Grutters, M., Van Raaphorst, W., Boer, W., Malschaert, H., Helder, W. Labile organic matter accumulation due to

resuspension and down slope transport on the Faeroe Shetland Channel, submitted for publication.

Gust, G., Michaels, A.F., Johnson, R., Deuser, W.G., Bowles, W., 1994. Mooring line motions and sediment trap hydromechanics: in situ intercomparison of three common deployment designs. Deep-Sea Research I 41, 831–857.

Hatcher, A., Hill, P., Grant, J., 2001. Optical backscatter of marine flocs. Journal of Sea Research 46, 1–12.

Jago, C.F., Bale, A.J., Green, M.O., Howarth, M.J., Jones, S.E., McCave, I.N., Millward, G.E., Morris, A.W., Rowden, A.A., Williams, J.J., 1993. Resuspension processes and seston dynamics, southern North Sea. Philosophical Transactions of the Royal Society London A343, 475–491.

Lampitt, R.S., 1985. Evidence for the seasonal deposition of detritus to the deep-sea floor and its subsequent resuspension. Deep-Sea Research 32 (8), 885–897.

Lampitt, R.S., Newton, P.P., Jickells, T.D., Thompson, J., King, P., 2000. Near-bottom particles flux in the abyssal northeast Atlantic. Deep-Sea Research II 47, 2051–2071.

Lohse, L., Kloosterhuis, R.T., de Stigter, H.C., Helder, W., Van Raaphorst, W., Van Weering, T.C.E., 2000. Carbonate removal by acidification causes loss of nitrogenous compounds in continental margin sediments. Marine Chemistry 69, 193–201.

McCave, I.N., 1986. Local and global aspects of the bottom nepheloid layers in the world ocean. Netherlands Journal of Sea Research 20, 167–181.

Monaco, A., Heussner, S., Courp, T., Buscail, R., Fowler, S.W., Millot, C., Nyfeller, F., 1987. Particle supply by nepheloid layers on the Northwestern Mediterranean Margin. In: Degens, E.T., Izdar, E., Honjo, S. (Eds.), Particle Flux in the Ocean. Mitteilungen aus dem Geologisch–Paleontologischen Institut der Universität Hamburg, pp. 109–125.

Monaco, A., Biscaye, P., Soyer, J., Pocklington, R., Heussner, S., 1990a. Particle fluxes and ecosystem response on a continental margin: the 1985–1988 Mediterranean ECOMARGE experiment. Continental Shelf Research 10, 809–839.

Monaco, A., Courp, T., Heussner, S., Carbonne, J., Fowler, S.W., Deniaux, B., 1990b. Seasonality and composition of particulate fluxes during ECOMARGE-I, western Gulf of Lions. Continental Shelf Research 10 (9/10/11), 959–987.

Morris, A.W., Bale, A.J., Howland, R.J.M., Mantoura, R.F.C., Woodward, E.M.S., 1987. Controls of the chemical composition of particles populations in a macrotidal estuary (Tamar estuary, UK). Continental Shelf Research 7, 1351–1355.

Oey, L.-Y., 1998. Eddy energetics in the Faeroe–Shetland Channel: a model resolution study. Continental Shelf Research 17 (15), 1929–1944.

Riegman, R., Kraay, G.W., 2001. Phytoplankton community structure derived from HPLC analysis of pigments in the Faeroe–Shetland Channel during summer 1999: the distribution of taxonomical groups in relation to physical/chemical conditions in the photic zone. Journal of Plankton Research 23 (2), 191–206.

Sherwin, T.J., 1991. Evidence of a deep internal tide in the Faeroe–Shetland Channel. In: Parker, B.P. (Ed.), Tidal Hydrodynamics. Wiley Interscience, Chichester, pp. 469–488.

Stoker, M.S., Hitchen, K., Graham, C.C., 1993. The geology of the Hebrides and West Shetland shelves, and adjacent deep-water areas. United Kingdom Offshore Regional Report, British Geological Survey, London.

Suess, E., 1980. Particulate organic carbon flux in the oceans–surface productivity and oxygen utilization. Nature 288, 260–263.

Thomsen, L., Gust, G., 2000. Sediment erosion thresholds and characteristics of resuspended aggregates on the western European continental margin. Deep-Sea Research I 47 (10), 1881–1897.

Thomsen, L., Van Weering, T.C.E., 1998. Spatial and temporal variability of particulate matter in the benthic boundary layer at the N.W. European continental margin (Goban Spur). Progress in Oceanography 42, 61–76.

Thorpe, S.A., White, M., 1988. A deep intermediate nepheloid layer. Deep-Sea Research 35 (9), 1665–1671.

Turell, W.R., Slesser, G., Adams, R.D., Payne, R., Gillibrand, P.A., 1999. Decadal variability in the composition of Faeroe Shetland Channel bottom water. Deep-Sea Research I 46, 1–25.

Vangriesheim, A., Khripounoff, A., 1990. Near-bottom particle concentration and flux: temporal variations observed with sediment traps and Nephelometer on the Meriadzek Terrace, Bay of Biscay. Progress in Oceanography 24, 103–116.

Van Raaphorst, W., Malschaert, H., Van Haren, H., 1998. Tidal resuspension and deposition of particulate matter in the Oyster Grounds, North Sea. Journal of Marine Research 56, 257–291.

Van Raaphorst, W., Malschaert, H., van Haren, H., Boer, W., Brummer, G.-J., 2001. Cross-slope zonation of erosion and deposition in the Faeroe–Shetland Channel, North Atlantic Ocean. Deep-Sea Research I 48 (2), 567–591.

Van Weering, T.C.E., de Stigter, H.C., 1999. Recent sediment transport and accumulation on the western Iberian Margin, Ocean Margin EXchange II Report, pp. 83–92.

Van Weering, T.C.E., McCave, I.N., De Stigter, H.C., Hall, I., Thomsen, L., 1998. Recent sediments, sediment accumulation and carbon burial at Goban Spur, NW European continental margin. Progress in Oceanography 42, 5–35.

Verardo, D.J., Froelich, P.N., McIntyre, A., 1990. Determination of organic carbon and nitrogen in marine sediments using the Carlo Erba NA-1500 analyzer. Deep-Sea Research 37 (1), 157–165.

Walsh, J.P., Nittrouer, C.A., 1999. Observations of sediment flux to the Eel continental slope, northern California. Marine Geology 154, 55–68.

Walsh, I., Fisher, K., Murray, D., Dymond, J., 1988. Evidence for resuspension of rebound particles from near-bottom sediment traps. Deep-Sea Research 35 (1), 59–70.

Wollast, R., 1991. The coastal organic carbon cycle: fluxes, sources and sinks. In: Mantoura, R.F.C., Martin, J.-M, Wollast, R. (Eds.), Ocean Margin Processes and Global Change. Wiley Interscience, Chichester, pp. 365–381.